15

Large-Eddy Simulation of Turbulent Flow and Plume Dispersion in a Spatially-Developing Turbulent Boundary Layer Flow

Hiromasa Nakayama
Japan Atomic Energy Agency
Japan

1. Introduction

In one of local-scale dispersion problems, we have an important issue in the accurate prediction of airborne contaminant dispersion from industrial or nuclear facilities for safety and consequence assessments of nuclear facilities. For evaluating radiological consequences of radioactive materials, it is need to predict not only the material concentration in the air at the evaluation point for internal dose but also on the three-dimensional distribution of the plume and surface deposition for external dose. In a flat terrain, time-averaged concentration of a plume can be easily predicted by a conventional Gaussian plume model. However, in Japan, most nuclear facilities are located in complex coastal terrain. Therefore, it is important to predict the spatial distribution of concentrations considering effects from terrain and buildings.

Another issue related to atmospheric dispersion in a local-scale is the potential problem that hazardous and flammable materials are accidentally or intentionally released into the atmosphere, either within or close to populated urban areas. For the assessment of human health hazards from such toxic substances, the existence of high concentration peaks in a plume should be considered because it is the instantaneous, not average, concentration that is fatal to humans. In such a situation, it is necessary to accurately predict the unsteady behavior of a plume, considering the effects of individual buildings. For the safety analysis of flammable gases, certain critical threshold levels should be evaluated. Therefore, in such a situation, not only the average levels but also instantaneous magnitudes of concentration should be accurately predicted.

There are various methods for predicting plume dispersion in atmospheric boundary layers, e.g. wind tunnel experiments and Computational Fluid Dynamics (CFD). It is well known that wind tunnel experiments are a rational tool for predicting plume dispersion behavior under local topography and/or building conditions. For the case of accidental or intentional release of contaminated materials within urban areas, many studies using a wind tunnel have been made to investigate the spatial extent of contaminated areas and the characteristics of mean and fluctuating concentrations around an individual building. In the safety assessment for the construction of nuclear facilities, prediction of the spatial distribution of radionuclide concentrations over complex terrain containing buildings is required by using a wind tunnel (*Meteorological Guide for Safety Analysis of Nuclear Power*

Plant Reactor, Nuclear Safety Commission of Japan, 1982). Although reliable data can be obtained on air flow and plume dispersion, wind tunnel experiments are time consuming, costly, and have limited availability for these applications. For example, in the safety assessment, experimental results are only used to derive the effective stack height, which is applied for long term assessment using a Gaussian plume model, and the effective stack height is usually determined lower height than the actual height considering terrain and building effects in a way that provides a conservative evaluation. On the other hand, recently the CFD technique has been proposed for use as an alternative to wind tunnel experiments (Sada *et al*., 2009) developed a numerical model for atmospheric diffusion analysis and evaluation of effective dose for safety analysis and showed its effectiveness in comparison with wind tunnel experiments.

The CFD technique has been recognized as a helpful tool with the rapid development of computational technology. The CFD technique uses computers to numerically predict fluid flow, heat transfer and mass transfer by solving the governing equations. In particular, there are two different approaches, the Reynolds-Averaged Navier-Stokes (RANS) and Large-Eddy Simulation (LES) models, which are both effective for predicting turbulent flows. In RANS, a mean wind flow is computed, delivering an ensemble- or time-averaged solution, and all turbulent motions are modeled with a turbulence model. The main advantage of the RANS model is its efficiency in computing a mean flow field with relatively low computational cost. Sada *et al*., (2009) designed a practical numerical model based on the RANS model.

Recently, LES has come to be regarded as an effective prediction method for environmental flows. LES resolves the large-scale turbulent motions and models only the smallest scale motions, which are usually more universal. Although the LES model requires larger computational costs than RANS model, it is no less useful the latter, considering the cost and limited availability of wind tunnels and the experimental time needed. Furthermore, LES can provide accurate predictions and detailed information about turbulence structures, and mean and fluctuating concentrations of a plume as well as wind tunnel experiments can provide them. Therefore, we have developed an LES dispersion model applicable to actual problems of atmospheric dispersion on a local scale. As a first step, we previously performed LES for turbulent flows and plume dispersion over a flat terrain (Nakayama & Nagai, 2009). When compared to experimental results of Fackrell & Robins., (1982), it was shown that turbulence structures, the characteristic mean and r.m.s. (root mean square) concentrations, turbulent concentration flux and peak concentration over a flat terrain are successfully simulated. These findings implied that our LES model could replace wind tunnel experiments for safety assessments of nuclear facilities and also provide detailed information for the consequence assessment of accidental and intentional releases of radioactive materials into the atmosphere.

For the second step, we apply our LES dispersion model to the complex behaviors of separated shear layers and large eddies in the near-wake of a building. First, we propose a scheme to generate a spatially-developing turbulent boundary layer flow with strong velocity fluctuations, which is applicable to various types of wind tunnel flows and perform an LES of plume dispersion around an isolated cubical building. Then, we examine basic performance of the model and scheme by comparing LES data of the turbulent structure and characteristics of mean and r.m.s. concentrations including peak concentration with experimental data.

2. Numerical model

The governing equations for LES of atmospheric flow are the filtered continuity equation, the Navier-Stokes equation,

$$\frac{\partial \overline{u}_i}{\partial x_i} = 0 \ , \tag{1}$$

$$\frac{\partial \overline{u}_i}{\partial t} + \overline{u}_j \frac{\partial \overline{u}_i}{\partial x_j} = -\frac{1}{\rho}\frac{\partial \overline{p}}{\partial x_i} + \frac{\partial}{\partial x_j}\nu\left(\frac{\partial \overline{u}_i}{\partial x_j} + \frac{\partial \overline{u}_j}{\partial x_i}\right) - \frac{\partial}{\partial x_j}\tau_{ij} + f_i \ , \tag{2}$$

$$\tau_{ij} = \overline{u_i u_j} - \overline{u}_i \overline{u}_j \ , \tag{3}$$

$$\tau_{ij} - \frac{1}{3}\delta_{ij}\tau_{kk} = -\nu_{SGS}\overline{S_{ij}} \quad \nu_{SGS} = \left(C_s f_s \overline{\Delta}\right)^2 \left(2\overline{S_{ij}}\,\overline{S_{ij}}\right)^{\frac{1}{2}} , \tag{4}$$

$$\overline{S_{ij}} = \left(\partial \overline{u_i}/\partial x_j + \partial \overline{u_j}/\partial x_i\right)/2 \ , \tag{5}$$

and

$$\overline{\Delta} = \left(\overline{\Delta_x}\,\overline{\Delta_y}\,\overline{\Delta_z}\right)^{\frac{1}{3}} \ , \tag{6}$$

where u_i, t, p, ρ, ν, τ_{ij} and f_i are the wind velocity, time, pressure, density, kinematic viscosity, subgrid-scale Reynolds stress and external force term, respectively. The subscript i stands for coordinates (1, streamwise; 2, spanwise; and 3, vertical direction). Over bars, ($\overline{\ }$) denote application of the spatial filter. δ_{ij}, ν_{SGS}, C_s and f_s are the Kronecker delta, the eddy viscosity coefficient, the model constant of the flow field and Van Driest damping function (Van Driest., 1956), respectively. $\overline{\Delta}$ denotes the grid-filter width. In this LES model, the external force term proposed by Goldstein *et al*., (1993) is applied because of its computational stability for turbulent flow around a bluff body. The force term, f_i is incorporated into the Navier-Stokes equation to consider the building effects and can be assumed as the following expression;

$$f_i = \alpha \int_0^t u_i(t')dt' + \beta u_i(t), \quad \alpha < 0, \ \beta < 0 \tag{7}$$

where a and β are negative constants. The stability limit is given by $\Delta t < \dfrac{-\beta - \sqrt{\left(\beta^2 - 2\alpha k\right)}}{\alpha}$ where k is a constant of order 1. The most commonly used sub-grid scale models are the standard and dynamic type Smagorinsky models (Smagorinsky., 1963; Germano *et al*., 1991; Lilly *et al*., 1992; Meneveau *et al*., 1996). Although C_s should be estimated depending on the flow type, the standard Smagorinsky model (Smagorinsky., 1963) with the Van Driest damping function is used instead in our LES model because of its simplicity and low computational cost. C_s is set to 0.12 (Shirasawa *et al*., 2008).

The LES of plume dispersion is also computed by using the standard Smagorinsky model. The spatially filtered scalar conservation equations are presented by

$$\frac{\partial \overline{c}}{\partial t} + \overline{u}_j \frac{\partial \overline{c}}{\partial x_j} = -\frac{\partial}{\partial x_j} s_j \,, \tag{8}$$

$$s_j = \overline{u_j c} - \overline{u}_j \overline{c} \tag{9}$$

and

$$s_j = -\frac{\nu_{SGS}}{Sc_{SGS}} \frac{\partial \overline{c}}{\partial x_j} \,, \tag{10}$$

where s_j is the subgrid-scale scalar flux which is also parameterized by an eddy viscosity model. The model constant, Sc_{SGS}, is the turbulent Schmidt number and it is set to a constant value of 0.5 (Sada & Sato., 2002).

The coupling algorithm of the velocity and pressure fields is based on the Marker and Cell (Harlow & Welch, 1965) method with the Adams-Bashforth scheme for time integration. The Poisson equation is solved by the Successive Over-Relaxation method that is an iterative method for solving a Poisson equation for pressure. For the spatial discretization in the governing equation of flow and the tracer transport, a second-order accurate central difference is used. For only the advection term in the dispersion field, the Cubic Interpolated Pseudo-particle (CIP) method (Takewaki *et al*., 1985; Yabe & Takei., 1988) is imposed in order to prevent a numerical instability. The CIP is a very stable scheme that can solve generalized hyperbolic equations in space. The Reynolds number based on the cubical building height and wind speed at the building height is almost 5,000.

3. Wind tunnel experiments for evaluating the model performance

Over the past few decades many wind tunnel experiments have been conducted on the dispersion characteristics of a plume in the near-wake of a cubical building. For example, Sada & Sato., (2002) conducted experiments under neutral atmospheric stratification in the wind tunnel of Central Research Institute of Electric Power Industry. The wind tunnel test section was 20m long, 3m wide and 1.5m high. An approaching flow with strong velocity fluctuations was generated using roughness elements with L-shaped cross sections placed on the floor at the entrance of the wind tunnel. It was shown that spanwise and vertical spreads of a plume corresponded to the Pasquill-Gifford stability class D. A plume was released from an elevated point source located upstream from the cubical building and concentration of the plume is measured by a fast-response flame ionization detector. The vertical profiles of mean wind velocity, turbulence intensity, mean and r.m.s. concentrations and peak concentration in the near-wake region of the cubical building were all obtained from the experiments. In this wind tunnel experiment, the building Reynolds numbers based on the cubical building height and wind speed at the building height is about 13,000.

In the present paper, in order to evaluate the model performance, we compare our LES results of turbulent flow and plume dispersion in the near-wake region of a cubical building with the wind tunnel experimental data of Sada & Sato., (2002).

4. Computational settings

In wind tunnel experiments, a neutral atmospheric turbulent boundary layer is simulated mainly using various types of obstacle, such as spires, tripping fences and roughness blocks. Therefore, various wind tunnel flows that have different turbulence characteristics can be obtained depending on the wind tunnel facility. In an LES study of turbulent flow in the atmosphere, an approach flow with turbulent fluctuations as the inlet boundary condition of the model domain should be generated depending on the target wind tunnel flow by a certain method.

In our LES model, the driver region for generating a spatially-developing turbulent boundary layer flow and the main region for simulating of plume dispersion around a cubical building immersed in a fully-developed turbulent boundary layer are set up. In this scheme, first a thick turbulent boundary layer flow is generated by incorporating the existing inflow turbulence generation method, that is, the method of Kataoka & Mizuno., (2002) into an upstream small fraction of the driver region as shown in Figure 1(a). Then, a strong wind velocity fluctuation is produced by a tripping fence placed downstream from the recycle station as shown in Figure 1(b).

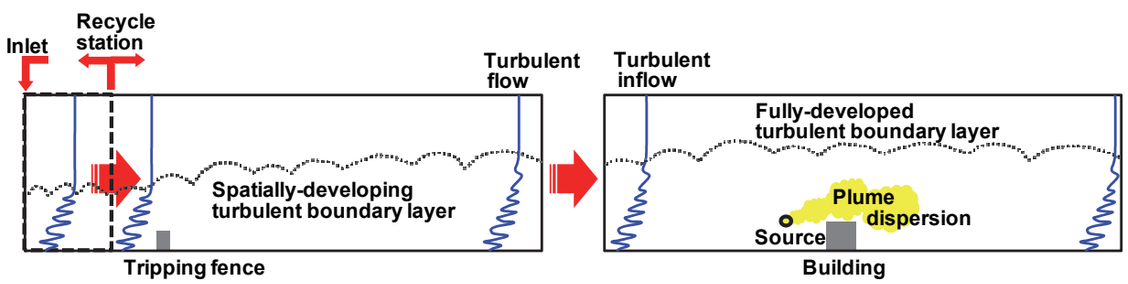

Fig. 1. Schematic of numerical model. (a) Driver region for generating turbulent boundary layer flow. (b) Main region for turbulent flow and plume dispersion around a cubical building.

In the method of Kataoka & Mizuno., (2002), the fluctuating part of the velocity at the recycle station is recycled and added to the specified mean wind velocity at each time interval by assuming that boundary layer thickness is constant within the driver section. This method requires a driver section with a length of about 1.0δ. The formulation of the method of Kataoka & Mizuno., (2002) is as follows.

$$u_{inlt}(y,z,t) = \langle u \rangle_{inlt}(z) + \phi(\theta)\left\{u_{recy}(y,z,t) - [u](z)\right\}, \tag{11}$$

$$v_{inlt}(y,z,t) = \phi(\theta)\, v_{recy}(y,z,t), \tag{12}$$

$$w_{inlt}(y,z,t) = \phi(\theta)\left\{w_{recy}(y,z,t) - [w](z)\right\}, \tag{13}$$

$$\phi(\theta) = \frac{1}{2}\left\{1 - \tanh\left[\frac{a(\theta - b)}{(1-2b)\theta + b}\right] \Big/ \tanh a\right\}, \tag{14}$$

Here, u_{inlt} and u_{recy} are the instantaneous wind velocity at the inlet and the downstream position (the recycle station), respectively. $\langle u \rangle_{inlt}$ is the specified mean wind velocity at the inlet. $[u_i]$ is the averaged wind velocity in the horizontal plane. $\phi(\theta)$ is a damping function to control the transport of turbulent fluctuation into the free stream. *a* and *b* are constants.

Calculations of both driver and main regions are done by the same model with different computational settings. As boundary conditions, the Sommerfeld radiation condition (Gresho., 1992) is imposed at the exit, a free-slip condition for streamwise and spanwise velocity components is imposed and the vertical velocity component is 0 at the top, a periodic condition is imposed at the side, and a non-slip condition for each velocity component is imposed at the ground surface. Here, in our LES model, we do not use wall functions as the boundary condition of the ground surface. Therefore, the resolution of a vertically stretched grid above the ground surface is set to 1.7 in order to resolve the viscous layer.

The size and the number of grid points for the driver region is 32.8H×10.0H×9.5H (H: height of the cubical building) and 410×120×70 in streamwise, spanwise and vertical directions, respectively. A tripping fence has a height of 0.45H.

The size and number of grid points for the main region are 18.9H×10.0H×9.5H and 400×120×70 in streamwise, spanwise and vertical directions, respectively. The cubical building is resolved by 20×20×30 grids in the streamwise, spanwise and vertical directions, respectively. According to numerical experiments of Xie *et al.*, (2006) and Santiago *et al.*, (2008), a building should be resolved by at least 15-20 grid points in each dimension in order to capture complex turbulent behaviors. The mesh number of the building set up in our LES model is enough to accurately simulate turbulent flows around a building. At the inlet of the main region, the inflow turbulence data obtained near the exit of the driver region is imposed at each time interval. In a concentration field, zero gradient is imposed at all the boundaries. The release point of a tracer gas is located 1.5H upstream from the center of the building and elevated at height, H. According to the above-mentioned coordinates, the location of the release point of a plume corresponds to x/H=0.0 and z/H=1.0 as seen in Figure 2.

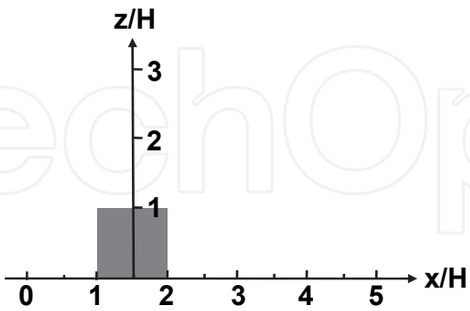

Fig. 2. Coordinate system.

5. Results

5.1 Approach flow

Figure 3 compares the LES model results with wind tunnel experimental data (Sada & Sato., 2002) of the vertical profiles of mean wind velocity (U), each component of turbulence

intensities (u', v', w') and Reynolds stress in the driver region. The turbulence statistics is normalized by a free-stream velocity (U_∞). We see that the mean wind velocity profile obtained by our LES model is consistent with the experimental data. Strong turbulent fluctuations are produced from the ground surface to the upper part of the boundary layer and each component of the LES-generated turbulent intensity profiles is found to be in good agreement with the experimental data. The Reynolds stress profile obtained by our LES model is also in good agreement with the experimental data.

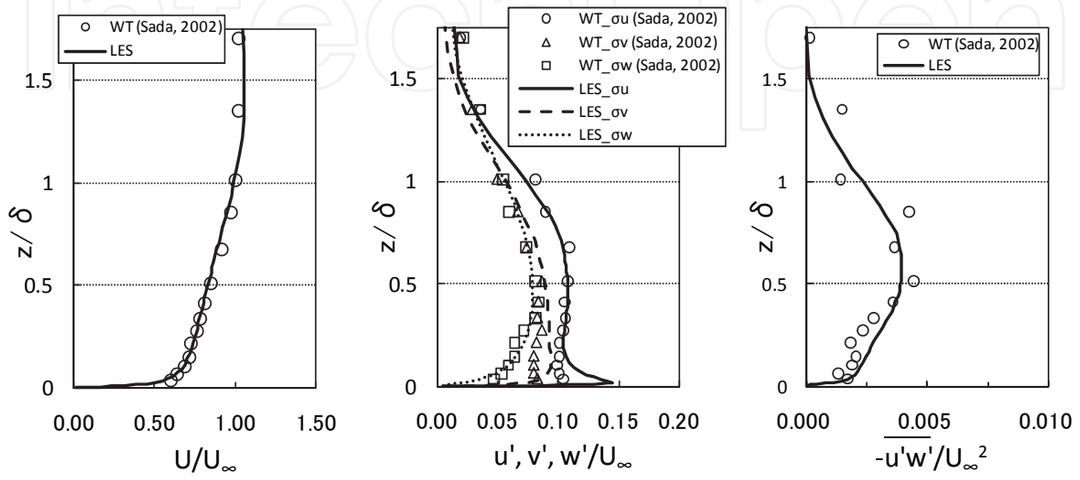

Fig. 3. Turbulence characteristics of approach flow.

5.2 Turbulent flow field

Figure 4 shows mean velocity vectors by LES around a building. The reattachment lengths of recirculating flow behind the building normalized by the building height of the experiments and the LES model is L/H=1.2 and 1.35 (L: reattachment length), respectively; the latter is slightly larger. Figure 5 shows a comparison of our LES model results with the experimental data (Sada & Sato., 2002) of the vertical profiles of mean wind velocity obtained downstream at x/H=0.0, 1.5, 2.5 and 3.5. The LES model results of mean wind velocity are consistent with the wind tunnel experimental data at each downwind position.

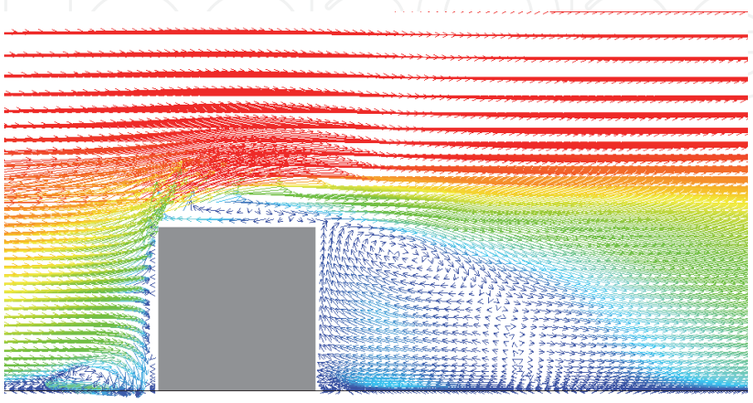

Fig. 4. Mean velocity vectors around a building.

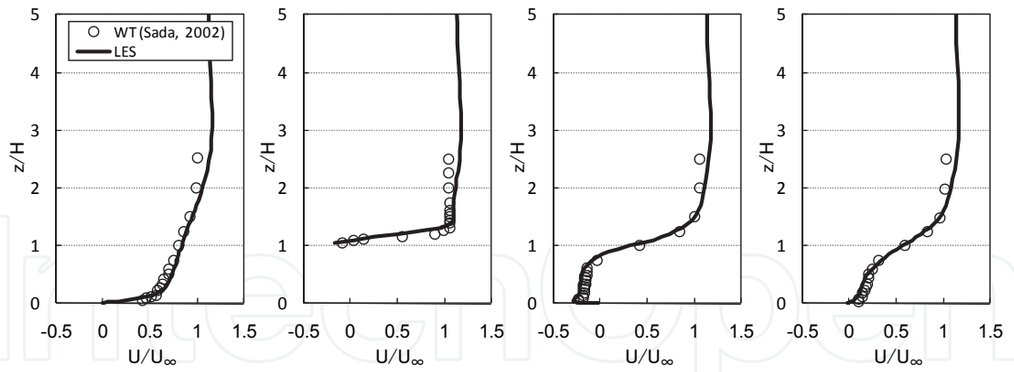

Fig. 5. Streamwise variation of vertical profiles of mean wind velocity.

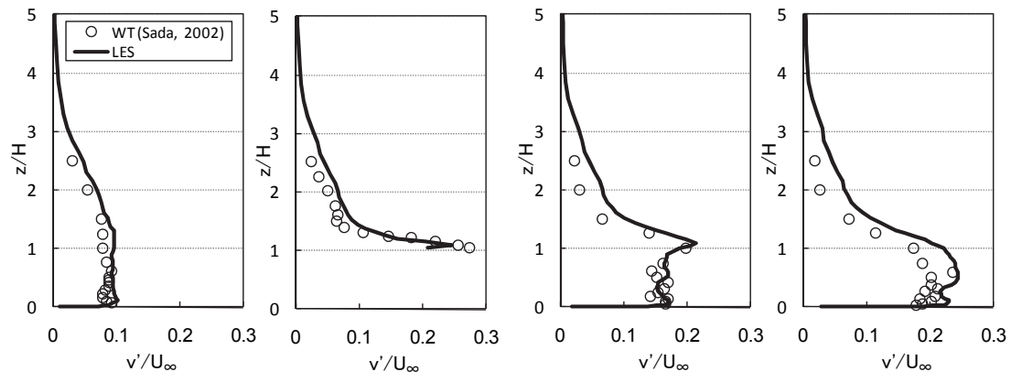

(a)

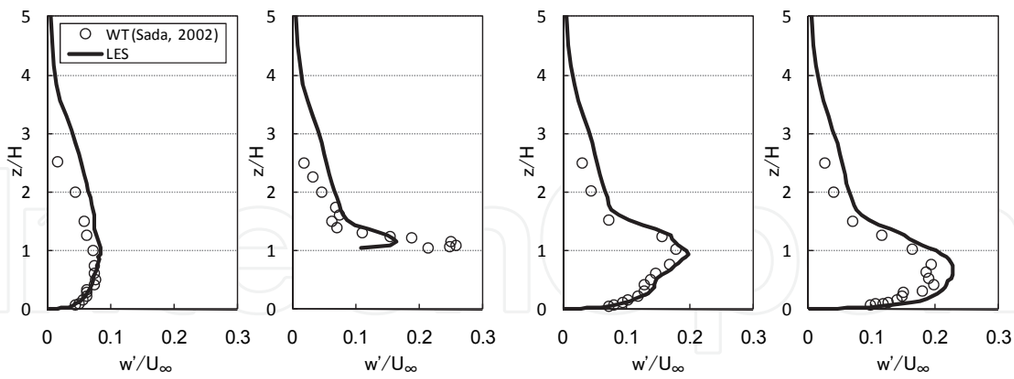

(b)

Fig. 6. Streamwise variation of turbulence intensities. (a) Horizontal turbulence intensity. (b) Vertical turbulence intensity.

Figure 6 shows a comparison of our LES model results with the wind tunnel experimental data of the vertical profiles of (a) horizontal and (b) vertical turbulence intensities normalized by free-stream velocity obtained downstream at x/H=0.0, 1.5, 2.5 and 3.5. Just above the roof of the building at x/H=0.0, the LES model results of both horizontal and vertical turbulence intensities are underestimated. At the position located away from the

building, x/H=3.5, the LES model results of both horizontal and vertical turbulence intensities around the building height are a little overestimated. Mochida *et al*., (1991) reported that the LES results of turbulence kinetic energy using the standard Smagorinsky model were overestimated around the upper edge of the recirculation zone of an obstacle in comparison with the wind tunnel experimental data. The overestimation of turbulence intensities of LES behind a building is due to the use of the standard Smagorinsky model.
Although the standard Smagorinsky model has the above problems, the main characteristics are obtained in our simulation. They include a sharp peak behind the building due to the strong instability of separated shear layers and the formation of a uniform turbulent flow field with downstream distance due to the active turbulent motions almost the same as in the experimental data of Sada & Sato., (2002). The slight overestimation of the reattachment length has also been reported in other LES calculations (Murakami *et al*., 1986). Therefore, our LES model with the conventional Smagorinsky model shows reasonable accuracy and satisfactorily results.

5.3 Dispersion field

Figure 7(a), (b) and (c) shows instantaneous plume dispersion fields around a building at times t* (=tU_∞/H) = 15, 45 and 90 after the plume release. The yellow areas on iso-surface indicate 0.01% of initial concentration. It shows that the plume is passed above the building roof at first, and then the plume is entrained into the wake region of a building. After enough time passing, the plume is found to be widely dispersed behind a building due to the active turbulent motions.
Figure 8 shows a comparison of our LES model results and the wind tunnel experimental data (Sada & Sato., 2002) of the vertical profiles of mean (C) and r.m.s. (c') concentrations obtained downstream at x/H=1.5, 2.5, 3.5 and 5.0 in the near-wake region of the cubical building. The mean and r.m.s. concentrations are normalized by free-stream velocity, the building height and the source strength (Q). In both mean and r.m.s. concentration fields, the peak values of the LES model near the point source are about 50% smaller than the wind tunnel experimental results, while the model results are in good agreement with the experimental data, particularly at the position x/H=5.0, located away from the point source. These large discrepancies near the point source are possibly due to a coarse grid resolution for the plume source.
In our LES model, a plume source is provided in one grid-cell. Thus, the size of the point source is determined by the grid resolution. Michioka *et al*., (2003) examined the sensitivity of the grid resolution for the point source by LES of a plume dispersion released from the point sources corresponding to 1.0 and 10 times the real diameters of the point source. As a result, they found that the peak values of mean and r.m.s. concentrations near the point source in a coarse grid resolution were 80% smaller than the wind tunnel experimental data, while those in a fine grid resolution were consistent with the experimental data. The plume source diameter in our LES model is about 5.5 times that of the real one. Considering the discrepancy of the plume source diameter between the LES model and the wind tunnel experiments, our results have the same tendency to underestimate near the point source as the LES results by Michioka *et al*. Therefore, if the plume source size corresponding to the real one is properly set in our LES model, the model results near the point source should be improved. However, a fine grid resolution is not appropriate for our purpose and target scale considering its computational cost. Except for this discrepancy, the basic characteristics, such as a sharp peak just behind the cubical building and the formation of

uniform profiles of mean and r.m.s. concentrations with downstream distance are similar to the experimental data.

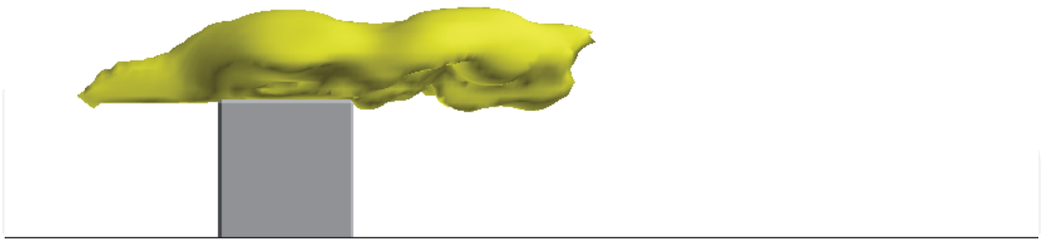

(a) t* =15

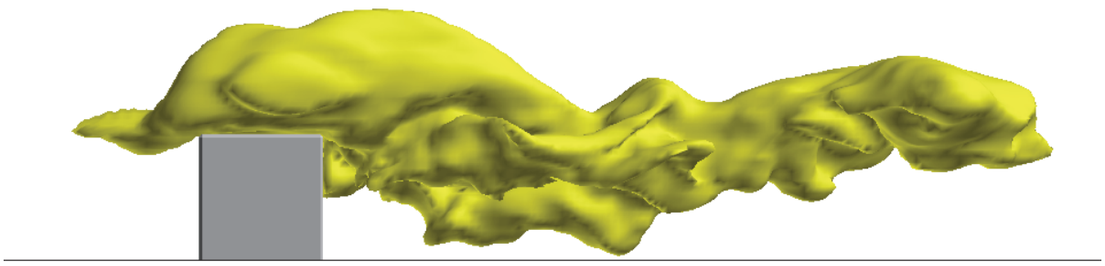

(b) t* =45

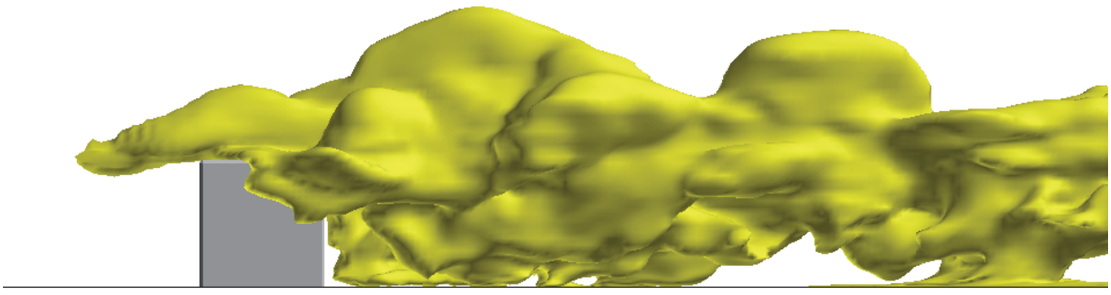

(c) t* =90

Fig. 7. Instantaneous plume dispersion field. The yellow areas on the isosurface indicate 0.01% of initial concentration.

In the present LES model, the point source diameter is larger than the real one because a numerical simulation with a fine grid resolution requires large computational time. However, as we explain above, our LES model presents almost the same patterns of concentration distributions as the wind tunnel experiments. This fact indicates that our LES model gives satisfacotoly results.

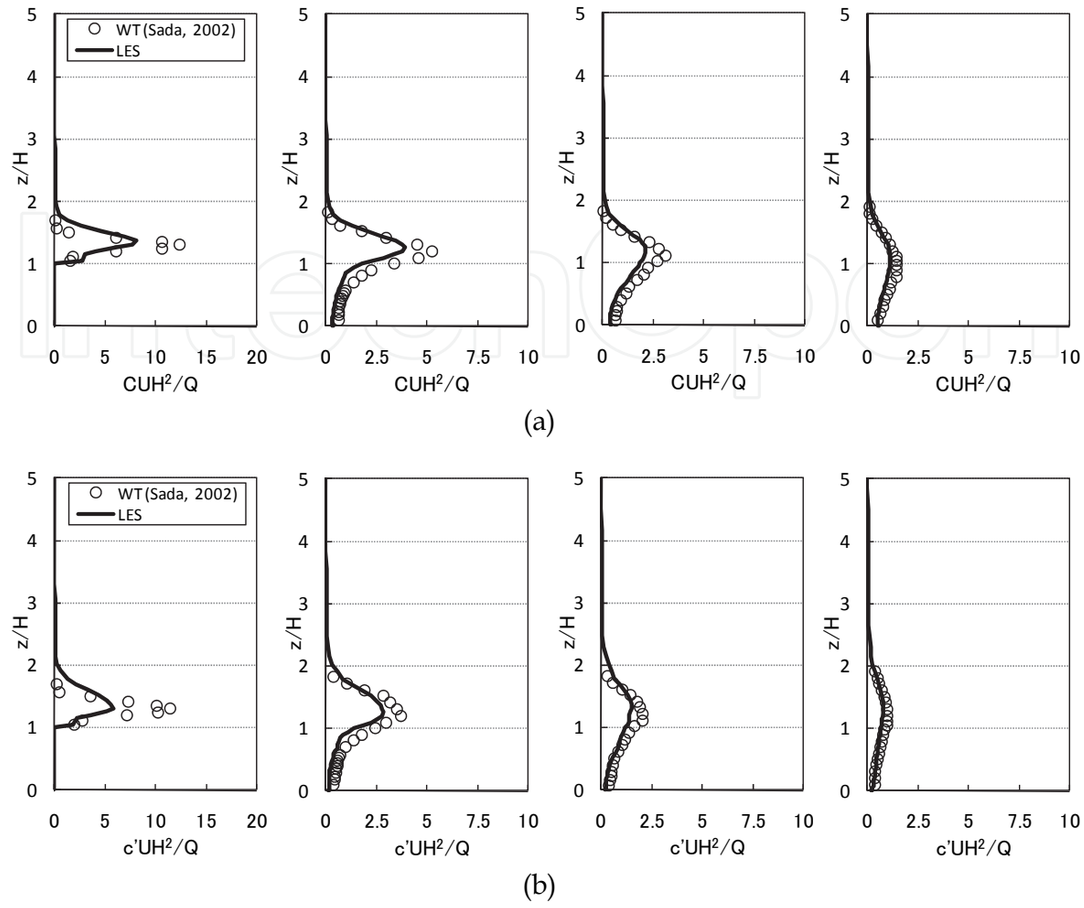

(a)

(b)

Fig. 8. Streamwise variation of vertical profiles of mean concentrations in the near-wake of the cubical building. (a) Mean concentration. (b) R.m.s. concentration.

5.4 Characteristics of the peak concentration

In case of accidental or intentional release of toxic or flammable gases into the atmosphere, it is important to estimate not only the mean but also the instantaneous and local peak concentrations near the surface of the ground. For example, Li & Meroney (1983) conducted wind tunnel experiments of gas dispersion of a plume released from the center roof vent of a cubical building and investigated the streamwise variation of vertical profiles of mean and r.m.s. concentrations, and various peak concentrations (c_{99}, c_{95}, c_{90}) defined as the values that are not exceeded for 99, 95, 90% of the cumulative probability density function in the near-wake region. In the theoretical studies of the probability distributions of concentration fluctuation have been studied by many researchers, Csanady (1973), Hanna (1984), and Lewellen & Sykes (1986) proposed theoretical models of the log-normal, exponential and clipped normal distributions for predicting concentration fluctuations of a plume in the atmosphere as follows.

Log-normal distribution function:

$$P(c) = \frac{1}{2}\left[1 + erf\left\{\frac{\ln(c/n_c)}{\sqrt{2}\sigma_l}\right\}\right], \tag{15}$$

Exponential distribution function:

$$P(c) = 1 - I\exp\left(-I\frac{c}{C}\right), \tag{16}$$

Clipped normal distribution function:

$$P(c) = \frac{1}{2}\left\{1 + erf\left(\frac{c-\mu_0}{\sqrt{2}\sigma_0}\right)\right\}, \tag{17}$$

Here, *erf*, n_c, σ_l, μ_0 and σ_0 are error function, the median concentration, the logarithmic standard deviation, the specified mean and the specified variance. According to Hanna (1984), I can be expressed as follows using C_i which is the concentration fluctuation intensity defined as the ratio of r.m.s. concentration to mean concentration.

$$I = \frac{2}{C_i^2 + 1}, \tag{18}$$

These theoretical models cannot predict the spatial distribution of concentration but can estimate peak concentrations at a stationary point. Sato and Sato., (2002) compared the log-normal, exponential and clipped normal probability distributions of concentration fluctuation in the near-wake region of a cubical building with those for wind tunnel experiments using concentration statistics of n_c, σ_l, C_i, μ_0 and σ_0 obtained in the experiments. They showed that a peak concentration of c_{99} could be predicted using the log-normal type for $0.3 < C_i < 1.0$, the log-normal or the exponential types for $1.0 < C_i < 1.5$, and the exponential type for $C_i > 1.5$, while peak concentration of the clipped-normal type was entirely underestimated.

Here, we first compare the probability distributions of concentration fluctuation of the LES model with those of the theoretical models and assess the prediction accuracy of the occurrences of instantaneous high concentrations in our LES model. Then, we examine the characteristics of not only peak concentration ratios of c_{99} but also c_{95} and c_{90} in the near-wake region of the cubical building.

Figure 9 shows a comparison of probability distribution functions (1-p(c)) of concentration fluctuation of the LES model at the heights of z/H=0.1, 1.6 and 2.0 at the downstream position of x/H=3.5 with theoretical model. Concentration is normalized with the r.m.s. concentration. Concentration fluctuation intensity, C_i, has values of 0.57, 1.3 and 2.2 at the heights of z/H=0.1, 1.6 and 2.0, respectively. For evaluating probability distributions of concentration fluctuation of each theoretical model, we use concentration statistics of n_c, σ_l, C_i, μ_0 and σ_0 obtained by the LES model. c_{99}, c_{95} and c_{90} are determined from 1-p(c)=0.99, 0.95 and 0.90, respectively. At z/H=0.1, the probability distribution of the LES model is almost the same as that of the log-normal type, while the model result of c_{99}/c' is much smaller than the exponential one. At z/H=1.6, the probability distribution of the LES model is similar to that of both the log-normal and exponential types. At z/H=2.0, the probability distribution of the LES model is consistent with that of the exponential type. Furthermore, the model results of c_{99}/c' are almost the same as those of the exponential one, while the log-normal probability distribution is different from that of the LES model. c_{99}/c' values obtained from the clipped-normal type are underestimated at each height. These facts

indicate that the characteristics of probability distributions of the LES model depending on the values of C_i are consistent with those reported by Sato & Sada., (2002). Therefore, the occurrences of instantaneous high concentrations are captured by LES and we conclude that the basic performance of the LES model for plume dispersion around the cubical building is nearly comparable to that for the wind tunnel experiments.

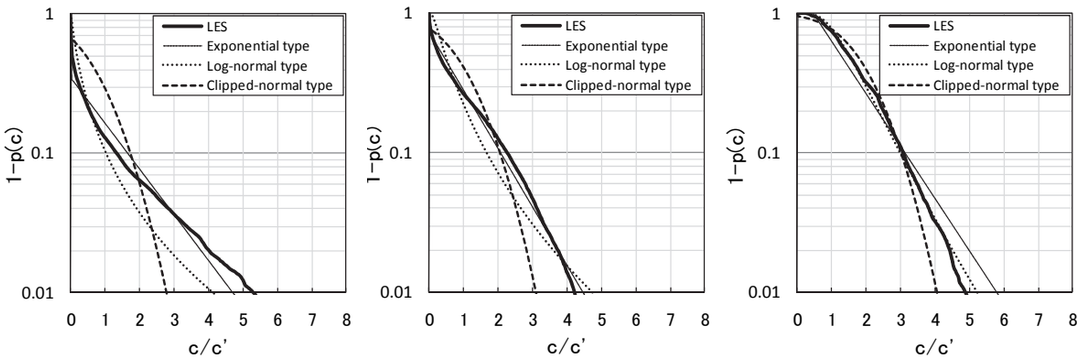

Fig. 9. Probability distribution functions of concentration fluctuation. (a)z/H=0.1, (b)z/H=0.16 and (c)z/H=2.0.

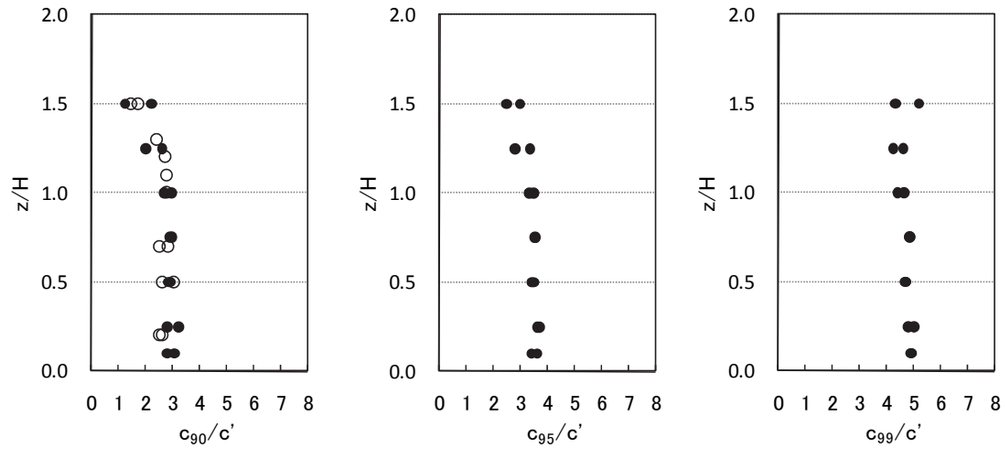

Fig. 10. Vertical profiles of various peak concentration ratios of (a)c_{90}/c', (b)c_{95}/c' and (c)c_{99}/c'.

Next, we examine various peak concentrations of c_{99}, c_{95}, and c_{90} obtained by the LES model. Figure 10 shows vertical profiles of various peak concentration ratios at x/H=2.5 and 3.5. c_{90}/c' values of the LES model have uniform distributions with a constant value of about 3.0 within the building height and gradually decrease above the building height. These tendencies are similar to the experimental data (Sada & Sato., 2002). c_{95}/c' of the LES model also shows a constant value of about 4.0 within the building height and slightly decreases above the building height. c_{99}/c' of the LES model provides uniform distributions with a constant value of about 5.0 at any position. This tendency is the same as the experimental data of Sato and Sato., 2002.

6. Conclusion

In this study, we performed LES of turbulent flow and plume dispersion around a cubical building and investigated the basic performance of the LES model in comparison with experimental data of Sada & Sato., (2002), Sato and Sato., (2002). The scheme to generate a spatially-developing turbulent boundary layer flow in the driver region was proposed by incorporating an existing inflow turbulence generation method into an upstream small fraction of the driver region with a tripping fence placed at the ground surface. With this scheme, we successfully simulated a turbulent boundary layer flow corresponding to that in wind tunnel experiments of Sada & Sato., (2002) in the driver section. The findings implied that our LES model could simulate various types of wind tunnel flow by incorporating the existing inflow turbulence generation method and moderately setting up roughness obstacles in the driver region.

Turbulence intensities behind a cubical building around the building height were slightly overestimated in comparison with experimental data of Sada & Sato., (2002). However, the main characteristics of turbulent flow such as a sharp peak behind the building and the formation of a uniform turbulent flow field with downstream distance, corresponding to the wind tunnel experiment, are obtained. Also, dispersion characteristics such as a sharp peak close to the point source and the formation of concentration profiles with downstream distance were successfully simulated in comparison with the experimental data. These indicated that the difference in turbulence characteristics between the experiments and our LES model was not significant. The basic performance of our LES model for turbulent flow and dispersion fields could be recognized as comparable to the wind tunnel experiment.

Dependence of the patterns of probability distributions of concentration fluctuation of the LES model on the values of concentration fluctuation intensity were consistent with those of the wind tunnel experimental results of Sato & Sada., (2002). Focusing on various peak concentration ratios, we saw c_{90}/c' and c_{99}/c' values of the LES model were in good agreement with the experimental data. From these facts, we considered that the occurrences of high concentrations were captured by our LES model. From the above results, we considered that the basic performance of our LES model was almost comparable level to that obtained by the wind tunnel experimental techniques.

Here, we discuss the applicability of the present LES model for flow and dispersion around an isolated building to the problem of plume dispersion within a group of buildings. Within an urban canopy, three typical flow patterns, isolated flow, wake interference flow and skimming flow within building arrays are formed depending on the ratio of the buildings height to the street width and the flow filed is highly complex (Oke., 1998). Considering a surface geometry of urban canopy is composed of a group of isolated buildings and obstacles, numerical simulation with moderate grid points for each building and obstacle can capture such complex flow patterns with reasonable accuracy. Therefore, from the validation of our LES model for turbulent flow and plume dispersion around an isolated building, it is considered that the present model with moderate grid points for each building can apply to a simulation of plume dispersion within urban canopy.

7. References

Csanady, G.T. (1973). *Turbulent Diffusion in the Environment*, D.Reidel Publishing Co., Dordrecht, Holland, 222-248

Fackrell, J.E. & Robins, A.G. (1982). Concentration fluctuation and fluxes in plumes from point sources in a turbulent boundary layer, *J. Fluid Mech.*, 117, 1-26

Germano, M.; Piomelli, U., Moin, P. & Cabot, W.H. (1991). A dynamic subgrid-scale eddy viscosity model, *Phys. Fluids.*, A3, 7, 1760-1765

Goldstein, D.; Handler, R. & Sirovich, L. (1993). Modeling a no-slip flow boundary with an external force field, *J. Comput. Phys.*, 105, 354-366

Gresho, P.M. (1992). Some interesting issues in incompressible fluid dynamics, both in the continuum and in numerical simulation, *Advances in Appl. Mech.*, 28, 45–140

Hanna, S.R. (1984). The exponential probability density function and concentration fluctuation in smoke plumes, *Bound.-Layer Meteor.*, 29, 361-375

Harlow, F. and Welch, J. E. (1965). Numerical calculation of time dependent viscous incompressible flow of fluid with a free surface, *Phys. Fluids.*, 8, 2182–2189

Kataoka, H. & Mizuno, M. (2002). Numerical flow computation around aeroelastic 3D square cylinder using inflow turbulence, *Wind and Struct.*, 5, 379-392

Lewellen, W.S. & Sykes, R.I. (1986). Analysis of concentration fluctuations from lidar observations of atmospheric plumes, *J. Appl. Meteor. Climatol.*, 25, 1145-1154

Li, W. & Meroney, R. (1983). Gas dispersion near a cubical model building. Part1. Mean concentration measurements, *J. Wind. Eng. Indust. Aero*, 12, 15-33

Li, W. & Meroney, R. (1983). Gas dispersion near a cubical model building. Part2. Concentration fluctuation measurements", *J. Wind. Eng. Indust. Aero.*, 12, 35-47

Lilly, D.K. (1992). A proposed modification of the Germano subgrid-scale closure method, *Phys. Fluids.*, A4, 3, 633-635

Meneveau, C.; Lund, T.S. & Cabot, W.H. (1996). A Lagrangian dynamic subgrid-scale model for turbulence, *J. Fluid Mech.*, 319, 353-385

Meteorological Guide for Safety Analysis of Nuclear Power Plant Reactor, Nuclear Safety Commission of Japan (1982).

Michioka, T.; Sato, A. & Sada, K. (2003). Large-Eddy Simulation for the tracer gas concentration fluctuation in atmospheric boundary layer, *Jpn. Soc. Mechanical Engineers, B*, 69 [680], 116-123

Mochida, A.; Murakami, S. & Hayashi, Y. (1991). Comparison between k-ε model and LES for turbulence structure around cube, *J. Environ. Eng.*, AIJ, 423, 23-31 (1991), [in Japanese]

Murakami, S.; Mochida, A. & Hibi, K. (1986). Three dimensional numerical simulation for air flow and building Part1 -Correspondence between prediction by large eddy simulation and wind tunnel experiment, *J. Architecture, Planning and Environ. Engi.*, AIJ, 360, 174-184[in Japanese]

Nakayama, H & Nagai, H. (2009). Development of local-scale high-resolution atmospheric dispersion model using Large-Eddy Simulation Part1: Turbulent flow and plume dispersion over a flat terrain, *J. Nuc Sci and Tech*, 46, 12, 1170-1177

Oke, T.R. (1998). Street design and urban canopy climate, *Energy and Buildings*, 11, 103-113

Sada, K. & Sato, A. (2002). Numerical calculation of flow and stack-gas concentration fluctuation around a cubical building, *Atmos. Environ.*, 36, 5527-5534

Sada, K.; Komiyama, S.; Michioka, T. & Ichikawa, Y. (2009). Numerical model for atmospheric diffusion analysis and evaluation of effective dose for safety analysis, *Trans. At. Energy Soc. Jpn.*, 8[2], 184-196

Santiago, J.L.; Coceal, O., Martilli, A. & Belcher, S, E. (2008). Variation of the Sectioanl Drag Coefficient of a Group of Buildings with Packing Density, *Bound.-Layer Meteor*, 128, 445-457.

Sato, A. & Sada, K. (2002). A wind tunnel experiment on tracer gas concentration fluctuation near a cubical model building, *J. Soc. Civil Engi.*, 706, 41-49, [in Japanese]

Shirasawa, T.; Endo, Y., Yoshie, R., Mochida, A. & Tanaka, H. (2008). Comparison of LES and Durbin type k-ε model for gas diffusion in weak wind region behind a building, *J. Environ. Eng.*, AIJ, 73 [627], 615-622[in Japanese].

Smagorinsky, J. (1963). General circulation experiments with the primitive equations, *Monthly Weather Review*, 91[3], 99-164

Takewaki, H.; Nishiguchi, A. & Yabe, T. (1985). Cubic Interpolated Pseudo-particle method (CIP) for solving hyperbolic-type equations, *J. Comput. Phys.*, 61, 261-268

Yabe, T. & Takei, E. (1988). A new higher-order Godunov method for general hyperbolic equations, *J. Phys. Soc. Jpn.*, 57[8], 2598-2601

Van Driest, E.R. (1956). On turbulent flow near a wall, *J. Aerospace Sci.*, 23, 1007-1011

Xie, Z.T.; Coceal, O. & Castro, I.P. (2008). Large-eddy simulation of flows over random urban-like obstacles, *Bound.-Layer Meteor.*, 129, 1-23

Computational Simulations and Applications

Edited by Dr. Jianping Zhu

ISBN 978-953-307-430-6
Hard cover, 560 pages
Publisher InTech
Published online 26, October, 2011
Published in print edition October, 2011

The purpose of this book is to introduce researchers and graduate students to a broad range of applications of computational simulations, with a particular emphasis on those involving computational fluid dynamics (CFD) simulations. The book is divided into three parts: Part I covers some basic research topics and development in numerical algorithms for CFD simulations, including Reynolds stress transport modeling, central difference schemes for convection-diffusion equations, and flow simulations involving simple geometries such as a flat plate or a vertical channel. Part II covers a variety of important applications in which CFD simulations play a crucial role, including combustion process and automobile engine design, fluid heat exchange, airborne contaminant dispersion over buildings and atmospheric flow around a re-entry capsule, gas-solid two phase flow in long pipes, free surface flow around a ship hull, and hydrodynamic analysis of electrochemical cells. Part III covers applications of non-CFD based computational simulations, including atmospheric optical communications, climate system simulations, porous media flow, combustion, solidification, and sound field simulations for optimal acoustic effects.

INTECH
open science | open minds

InTech Europe
University Campus STeP Ri
Slavka Krautzeka 83/A
51000 Rijeka, Croatia
Phone: +385 (51) 770 447
Fax: +385 (51) 686 166
www.intechopen.com

InTech China
Unit 405, Office Block, Hotel Equatorial Shanghai
No.65, Yan An Road (West), Shanghai, 200040, China
中国上海市延安西路65号上海国际贵都大饭店办公楼405单元
Phone: +86-21-62489820
Fax: +86-21-62489821

IntechOpen